Examples of prestack depth migration in TI media

Robert J. Ferguson and Gary F. Margrave

ABSTRACT

Wave field extrapolation by nonstationary phase shift can be formulated to allow velocity variation with both wavenumber and position, and so can accommodate anisotropic effects in highly inhomogeneous media. The examples presented use physical data, acquired at The University of Calgary in the Department of Geology and Geophysics modeling facility. The first represents a zero-offset recording in which the target geology is a reef edge underlying an anisotropic medium with a non-vertical axis of symmetry. Isotropic migration incorrectly positions the reef edge by 350 meters laterally. Anisotropic migration correctly positions the reef.

The second example is an anisotropic thrust sheet embedded in an isotropic medium. The sheet is made up of 4 separate blocks of a common anisotropic material with different axes of TI symmetry. The model is anisotropic and strongly heterogeneous. Two seismic lines were acquired; a constant source/geophone geometry (approximately zero offset), and a prestack geometry (split spread). Using isotropic migration neither data set could correctly image the model - especially the base of the model and reflections internal to the anisotropic thrust. Using anisotropic migration by nonstationary phase shift both data sets correctly image the model.

The extra cost in computer run time relative to isotropic migration is about 20%. Distribution of the TI thrust migration (prestack) over a number of computers reduced the run time by a factor proportional to the number of PCs.

INTRODUCTION

The notion that seismic anisotropy is intrinsic to wavefield propagation in the subsurface is swiftly gaining recognition as a factor in imaging. Though anisotropy is reported throughout the earth's' crust and upper mantle (Crampin, 1984) the special case of transverse isotropy (TI) is sufficiently common to warrant consideration (Byun, 1984). One of the most mathematically tractable forms of anisotropy, TI describes a medium in which a large number of homogeneous, isotropic layers are arranged in alternating planes. Five elastic parameters provide a complete description of the larger scale elastic properties of the medium (Postma, 1955).

Thomsen (1986) points out the fundamental inconsistency of trying to image an anisotropic subsurface using the assumption of isotropy. Authors such as Uzcategui (1995) and Kitchenside (1991) propose algorithms to image TI media. Their algorithms are based on ω - x extrapolation techniques which Margrave and Ferguson (1997) and Black et al. (1984) point out are space domain approximations to a nonstationary Fourier operator. Le Rousseau (1997) has extended Kitchenside's concepts to laterally varying media using a modified PSPI technique. Authors such as Margrave and Ferguson (1997), Wapenaar (1994) and Black et al. (1984) show that a wavefield extrapolation scheme can be formulated in Fourier space, that can cope

Contents

with lateral velocity variation. Margrave and Ferguson (1997) refer to this scheme as NSPS (nonstationary phase shift).

This paper presents an extension of nonstationary extrapolators to handle TI media for both zero-offset and prestack acquisition geometries. This is done without restriction on velocity gradient or TI axis of symmetry, and without restricting the strength of the anisotropy. Thomsen parameters are used to describe the anisotropy. Examples are presented that illustrate the ability of anisotropic migration to improve seismic images relative to isotropic migration.

NONSTATIONARY PHASE SHIFT

Using the model of exploding reflectors, a zero-offset equation for phase shift migration is a direct outcome of the linear theory of nonstationary filters (Margrave, 1998, Ferguson and Margrave, 1998) is

$$r(x_{\Delta z}) = \int \psi(x) W(x_{\Delta z}, x_{\Delta z} - x) dx \tag{1}$$

where $r(x_{\Delta_a})$ is an estimate of the reflectivity at depth Δz, x_{Δ_z} and x are respectively the horizontal coordinate at depth Δz and the horizontal at depth 0. Wavefield $\psi(x)$ is the coincident source/geophone input, and $W(x_{\Delta_z}, x_{\Delta_z} - x)$ is a wavefield extrapolator. A reflectivity estimate can be made at Δz by averaging all frequencies (Ferguson and Margrave, 1998). (Quantities ψ and W depend on temporal frequency ω though this notation is suppressed for simplicity.) Equation (1) corresponds to a spatial domain *combination* filter which Margrave and Ferguson (1997) call the limiting form of PSPI. There is an alternate form where the extrapolator W has dependence on x in it's first coordinate and is, what Margrave (1998) calls, a *convolution* filter. (Ferguson and Margrave (1998) derive a hybrid operator which Margrave and Ferguson (1998) show, due to it's symmetry, has greater stability than either of it's component forms.)

Migration of a single source gather $\psi(x, x_s)$ is detailed in Ferguson and Margrave (1998) and is given by

$$r(x_{\Delta z}, x_s) = W(x_s, x_{\Delta z} - x_s) \int \psi(x, x_s) W(x_{\Delta z}, x_{\Delta z} - x) dx \tag{2}$$

The reflectivity r is unique for each source coordinate x_s, similarly for the input wavefield ψ. Equation (2) corresponds to the migration of a single source gather, and the migration of many sources is simple to implement on a large number of processors.

Both zero-offset and prestack migration (equations 1 and 2) share the same extrapolator W. In the following examples W was applied in the Fourier domain using

$$\int \psi(x) W(x_{\Delta z}, x_{\Delta z} - x) dx = \int \left[\int \varphi(k_x) A(k_{\Delta z} - k_x, k_x) dk_x \right] \exp(-ik_{\Delta z} x_{\Delta z}) dk_{\Delta z} \tag{3}$$

where, $\varphi(k_x)$ is the forward Fourier transform of $\psi(x)$.

Contents

$$\varphi(k_x) = \int \psi(x) \exp(ik_x x) dx \quad . \tag{4}$$

The Fourier domain extrapolator A is related to W by

$$A(\delta k_x, k_x) = \frac{1}{2\pi} \int \alpha(x_{\Delta z}, k_x) \exp(i \delta k_x x_{\Delta z}) dx_{\Delta z} \tag{5}$$

where $\delta k_x = k_{\Delta_z} - k_x$. The nonevanescent form of α is

$$\begin{aligned} \alpha(x_{\Delta z}, k_x) &= \int W(x_{\Delta z}, \delta x) \exp(ik_x \delta x) d\delta x \\ &= \exp\left(i \Delta z \sqrt{\frac{\omega^2}{v(x_{\Delta z})^2} - k_x^2} \right) \end{aligned} \tag{6}$$

where $\delta x = x_{\Delta_z} - x$.

In zero-offset migration the velocity term v in equation (6) is halved to conform to the model of exploding reflectors.

W in equation (6) is a function of laterally variable velocity $v(x)$ thus it is nonstationary. We propose that velocity variation be extended by allowing $v(x)$ to become $v(x, k_x)$. Then equation (6) becomes a wavefield extrapolator that varies velocity with position and phase angle

$$\alpha(k_x, x) = \exp\left[i \Delta z \sqrt{\frac{\omega^2}{v(x)^2} - k_x^2} \right] \Rightarrow \exp\left[i \Delta z \sqrt{\frac{\omega^2}{v(x, k_x)^2} - k_x^2} \right]. \tag{7}$$

In the following source gather migrations the source extrapolator W (x_s, x_{Δ_z}-x_s) is approximated using an NMO correction applied as a temporal phase shift. The resulting reflectivity estimates in each migrated source gather are most accurate for positions directly beneath the source and decrease in accuracy for positions further away. In isotropic migrations the NMO corrections are calculated using rms velocities computed from surface at the location beneath the source. A more accurate source wavefield extrapolator is under development.

TI NONSTATIONARY PHASE SHIFT

Velocity $v(x,k_x)$ in equation (7) is the phase velocity for a Fourier plane wave determined by k_x and ω. A major strength of the phase-shift approach, compared to time domain Kirchhoff methods, is that only phase velocity is required. A complicating factor is the determination of the horizontal wavenumber dependence of velocity from theoretical descriptions that depend on angular direction.

The angle dependant velocities of a TI media can be completely described by five elastic constants whose mathematical forms are well established. However, these constants are difficult to interpret physically. Thomsen (1986) derives the five elastic constants such that two of them are the physically realizable values of P-wave velocity (α_o) and S-wave velocity (β_o), measured at zero offset, plus three additional

Contents

constants ε, δ^* and γ. For P-wave propagation the number of parameters reduces to four. We adopt the Thomsen (1986) derivations as input parameters for wavefield extrapolation (we do not use the weak form of Thomsen's equations).

P-wave velocity as a function of angle of incidence θ (Thomsen, 1986) is

$$v_p(\theta) = \alpha_o^2 \left[1 + \varepsilon \sin^2\theta + D^*(\theta)\right] \tag{8}$$

with

$$D^* = \frac{1}{2}\left[1 - \frac{\beta_o^2}{\alpha_o^2}\right]\left\{\left(1 + \frac{4\delta^*}{1 - \frac{\beta_o^2}{\alpha_o^2}}\sin^2\theta\cos^2\theta + \frac{4\left[1 - \frac{\beta_o^2}{\alpha_o^2} + \varepsilon\right]\varepsilon}{\left(1 - \frac{\beta_o^2}{\alpha_o^2}\right)^2}\sin^4\theta\right)^{\frac{1}{2}} - 1\right\}. \tag{9}$$

Each of the anisotropic parameters in equations (8) and (9) are functions of input position *x*, thus, we have five numerical fields of anisotropic parameters to specify, plus a field for the axes of symmetry.

TI MIGRATION

Wavefield extrapolation by phase shift through one depth step, Δ*z*, is an operation that loops over frequency; one monochromatic wavefield is extrapolated per loop. At all times during extrapolation k_x and ω are known; but in the anisotropic case, it is difficult to directly measure the angle of incidence of the incoming waves. A way to relate k_x and ω to angle of incidence θ is to compute a set of horizontal slownesses (*p*) for a range of evenly spaced angles (θ) using anisotropic velocities (Kitchenside, 1991). (For a non-zero symmetry axis, care must be taken to relate the angle of incidence of waves to the rotated axis of anisotropy.) From Snell's law,

$$p(x,\theta) = \frac{\sin(\theta)}{v(x,\theta)}. \tag{10}$$

Then θ as a function of *p* can be established using an interpolating polynomial,

$$\theta(p) = a_0 + a_1 p + a_2 p^2 + \ldots + a_n p^n \tag{11}$$

where a_i are the coefficients of an interpolating polynomial of order *n*, and p^i are increasing powers of horizontal slowness (computed using equation 10). Note that *p* can be given in terms of k_x and ω

$$p = \frac{k_x}{\omega}. \tag{12}$$

Given the coefficients a_i, equation (10) can be substituted into equation (11):

Contents

$$\theta\left(\frac{k_x}{\omega}\right) = a_0 + a_1\frac{k_x}{\omega} + a_2\left[\frac{k_x}{\omega}\right]^2 + \ldots + a_n\left[\frac{k_x}{\omega}\right]^n . \tag{13}$$

Thus, since k_x and ω are known at all points during the extrapolation process, an angle of incidence can be computed for each wave using equation (13). The corresponding P-wave velocities can then be computed using equations (8) and (9). Vertical slowness q is then given by

$$q(x,\theta) = \frac{\cos(\theta)}{v(x,\theta)} . \tag{14}$$

For the non-evanescent region the q values from equation (14) are used to calculate the values of the vertical wavenumbers

$$k_z = \omega q . \tag{15}$$

The form of the nonstationary extrapolator from equation (4) then becomes

$$\alpha(k_x, x, \omega) = \exp ik_z\Delta z \tag{16}$$

where,

$$k_z = \omega q(x, \theta(k_x, \omega)) . \tag{17}$$

Anisotropic depth migration for zero-offset data then proceeds in the usual recursive manner with the anisotropic extrapolator (equation 7) and, for the Fourier domain expression of combination migration, using equation (3). Anisotropic depth migration for source gathers proceeds, again in the Fourier domain, by applying the anisotropic combination filter to the traces recursively, then shifting them in an offset dependent manner after recursion. In the following examples the simple NMO process for equivalent media described previously is used. Note that the source correction is not applied recursively, but is applied directly from the surface for each depth level.

EXAMPLES

Isotropic reef with an anisotropic overburden

This section presents depth migrations of two physical model experiments – both acquired at the physical modeling facility at The University of Calgary. The first (figure 1a) was designed to represent a reef edge underlying a TI media. The TI media has a single axis of symmetry, 45 degrees measured from normal to the bedding of the material, and the media containing the reef is isotropic. Though not a nonstationary problem (the anisotropy is laterally invariant) the reef model is a good example of the need for anisotropic imaging. Figure (1b) shows a zoomed image of the zero-offset section data. Migration of the zero-offset section by isotropic phase shift yields an image of the reef edge which is displaced by about 350 m to the left of

Contents

it's true position (figure 2a). Migration by TI phase shift correctly positions the edge of the reef (figure 2b).

Anisotropic thrust sheet in an isotropic background

The second migration example is that of a flat reflector overlain by a TI thrust sheet embedded in an isotropic background, and represents a true anisotropic/nonstationary problem (the anisotropic parameters vary in the lateral coordinate). The thrust sheet is composed of four blocks (figure 3a) - each with a unique axis of symmetry (the zero-offset section is given in figure 3b). Migration of the zero-offset data by nonstationary phase shift (isotropic), yields a migrated image where reflectors within and below the TI material are incorrectly positioned (figure 4b). In particular the basement reflector exhibits substantial pull up. Migration by nonstationary phase shift (TI) does a better job of positioning the reflectors (Figure 4a), and has nearly flattened the basement reflector.

Notable in the migrated image is the apparent no data zone beneath the steepest two blocks of the thrust. The crossing energy at the base reflector between 2000 and 3300m is believed to indicate a shadow zone caused by the high-velocity thrust sheet overlying slower material. The shadow zone is a result of the zero-offset geometry of the recording. A normal incidence ray from the flat lying reflectors beneath the thrust tends to strike the hanging wall at an angle greater than the critical angle, so that zero-offset reflections from the area beneath the steep thrust blocks are not possible for nonevanescent energy.

Migration of the prestack data by anisotropic source-gather migration correctly positions the base reflector and fills in the shadow zone due to the multiplicity of ray paths afforded by the prestack geometry (figure 5a). Again, as can be seen in figure 5b, error due to using an isotropic migration (this time isotropic prestack) is evident in the incorrect positioning of the base reflector.

An example of the migration of a single source gather is given in figures 6a through 6d. The intermediate wavefields (figures 6b and c) show the process by which reflectors gradually focus on their way to the top of the section (t = 0) where they are output to image space.

Using a simple NMO correction for the downward continuation of the source causes an offset dependent error in the migrated source gather. The reflectivities directly beneath the source will be correctly imaged but less so with increased offset. On the geophone side, downward continuation proceeds as a nonstationary filter. Accuracy is limited only by run time, very fast for smooth models, very slow for complex models (Ferguson and Margrave, 1997). If the velocity variation is extremely strong there may also be stability problems (Margrave and Ferguson, 1998). Future source-gather migrations will incorporate an improved source extrapolator.

COMPUTER CONSIDERATIONS

Source-gather migrations were computed in a new computer lab at The University of Calgary. Available are 24 Pentium PCs with 128 megabytes of memory each. Fourteen PCs have 233 MHz processors while 10 have 300 MHz processors. One source gather in the anisotropic thrust data set above consists of, after padding, 256 traces and 512 samples per trace (4 ms sample rate). There are 86 source gathers acquired at 60 m intervals along the line. The required TI model is first constructed with 5 anisotropic parameters specified every 20 m in lateral coordinate, and every 10 m in depth. To ensure reasonable run times the model is smoothed and desampled in lateral coordinate and depth. (Nonstationary filters applied entirely in the Fourier domain run faster with smooth models).

Desampling is accomplished using RMS calculations in both spatial dimensions. Here each output coordinate, in the desampled model, is an RMS value computed using the eight neighboring samples laterally and four neighboring samples vertically. Only Vp and Vs are smoothed in this way. The other TI parameters are desampled without smoothing. The error caused by this use of the RMS method is not yet quantified. The resulting vertical sample rate of the model (figure 3a) is 40 m (split-step phase-shift migration is used to interpolate the output back to 10 m in depth). The horizontal sample rate of the model is 160 meters. The resulting smooth model consists of 56 by 32 samples.

The above rationale for desampling comes from access restrictions to the computer lab. Nighttime blocks of about 8 hours are generally available. A 300 MHz PC requires about 75 minutes and 267 megaflops to TI migrate one source gather, while a 233 MHz PC requires about 97 minutes. Thus the 86 source gather migrations require 5.3 days of run time. The extra cost of TI migration over isotropic migration is about 15 minutes per source gather on the 300 MHz PC and about 20 minutes on the 233 MHz PC (20%).

To meet the 8-hour limit, migration of the anisotropic thrust model was distributed over the 24 PCs in the new lab. Unfortunately, distribution of source gathers did not consider speed differences in the processors (they were assumed to be the same) thus optimal use of the lab was not made. Each machine was given 3 or 4 source gathers and a set of the required software (Matlab source code) by FTP. Distributing the 5.3-day run time reduced the actual wait time to about 6 hours. Interpretation of the migrated source gathers can be done individually or by binning into common offset sections.

For comparison a similarly designed and distributed stationary/isotropic source-gather migration required only 3.4 hours to migrate all 86 gathers. However, each nonstationary migration (run with the 56 by 32 model) is equivalent to computing 32 stationary migrations/source gather - needing 4.5 days of run time. Each stationary phase-shift migration can then be modified to accept anisotropic velocities at an extra cost of about 20%. The required run time then increases to 5.4 days - not including the overhead required to assemble 32 migrations/source into single images.

CONCLUSIONS

Depth migration by nonstationary phase shift allows velocity variation with both wavenumber and position, and so can image highly inhomogeneous media. Depth migration of TI physical models demonstrates the utility basing an imaging algorithm on nonstationary filter theory. The extra cost of allowing TI anisotropy compared to a similarly implemented isotropic migration is about 20%. Distribution of a prestack depth migration over a number of processors reduces run time by a factor proportional to the number of processors.

ACKNOWLEDGEMENTS

The authors would like to thank Dr. Don Lawton, Dr. Helen Isaac, Jennifer Leslie, Eric Gallant and the sponsors of CREWES for their assistance in this work.

REFERENCES

Black, J. L., Su, C. B., Wason, C. B., 1984, Steep-Dip depth migration: Expanded abstracts, **54**th Annual Mtg. Soc. Expl. Geophy., 456-457.

Byun, B. B., 1984, Seismic parameters for transversely isotropic media: Geophysics, **49**, 1908-1914.

Crampin, S., 1984, Anisotropy in exploration seismics: First Break, 19-21.

Ferguson R. J., and Margrave, 1998, A nonstationary description of depth migration: CREWES Research Report, **10**, Chapter 41.

Ferguson R. J., and Margrave, 1997, Algorithm comparisons for nonstationary phase shift: CREWES Research Report, **9**, Chapter 31.

Kitchenside, P. W., 1991, Phase shift-based migration for transverse isotropy: **61**tst Mtg., Soc. Expl. Geophys., Expanded Abstracts, 993-996.

Le Rousseau, J. H., 1997, Depth migration in heterogeneous, transversely isotropic media with the phase-shift-plus-interpolation method: **67**th Mtg., Soc. Expl. Geophys., Expanded Abstracts, 1703-1706.

Margrave, G. F., 1998, Theory of nonstationary linear filtering in the Fourier domain with application to time variant filtering: Geophysics, **63**, 244-259.

Margrave, G. F., and Ferguson, R. J., 1997, Wavefield extrapolation by nonstationary phase shift: **67**th Mtg., Soc. Expl. Geophys., Expanded Abstracts, 1599-1602.

Margrave, G. F., and Ferguson, R. J., 1998Explicti Fourier wavefield extrapolators: CREWES Report, Vol., **10**, chapter 39**.**

Postma, G. W., 1955, Wave propagation in a stratified medium: Geophysics, **20**, 780-807.

Thomsen, L., 1986, Weak elastic anisotropy: Geophysics, **51**, 1954-1966.

Uzcategui, O., 1995, 2-D depth migration in transversely isotropic media using explicit operators: Geophysics, **60**, 1819-1829.

Wapenaar, C. P. A., 1992, Wave equation based seismic processing: In which domain?: EAGE **54**th Conference Extended Abstracts, B019.

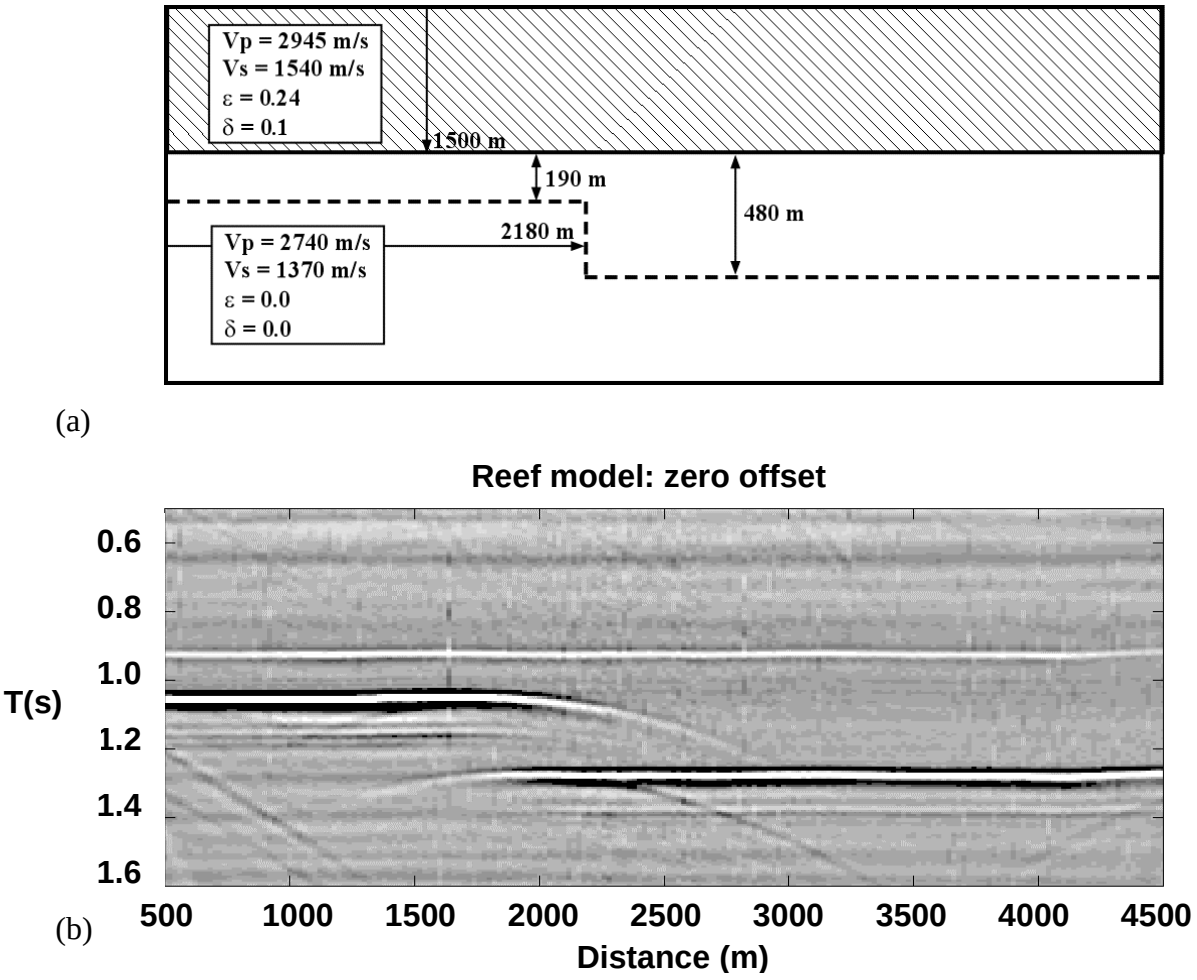

Fig.1. Model of an isotropic reef with an anisotropic overburden. (a) Dimensions and elastic parameters of the reef model. The axis of TI symmetry is +45 degrees. (b) Seismic data acquired with coincident source and receiver (the true offset scales to about 200 m).

Contents

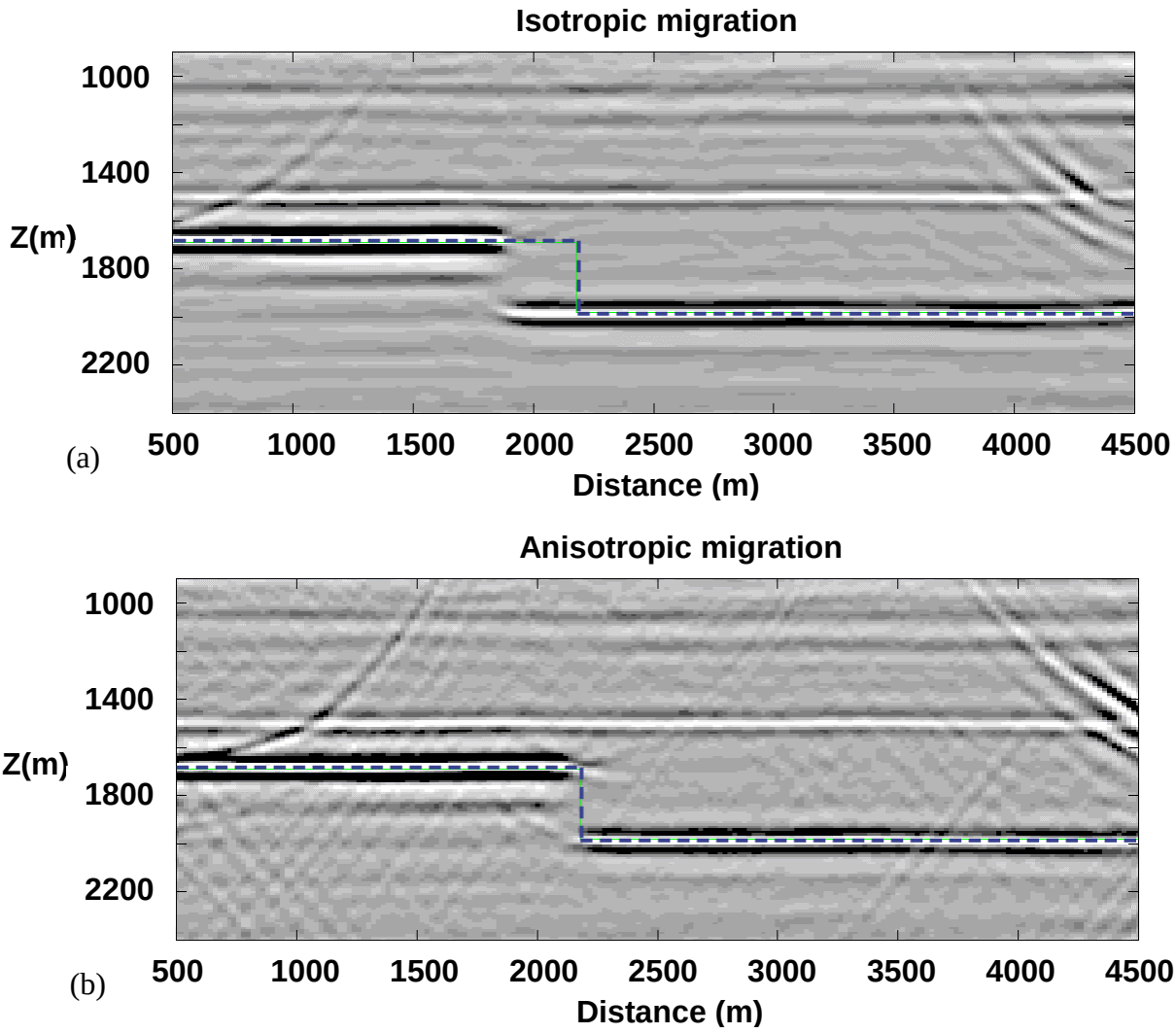

Fig.2. Migrations of figure 1a. (a) Isotropic phase-shift migration images the reef edge ~ 350 m left of its true position. (b) Anisotropic phase shift provides a correct image.

Contents

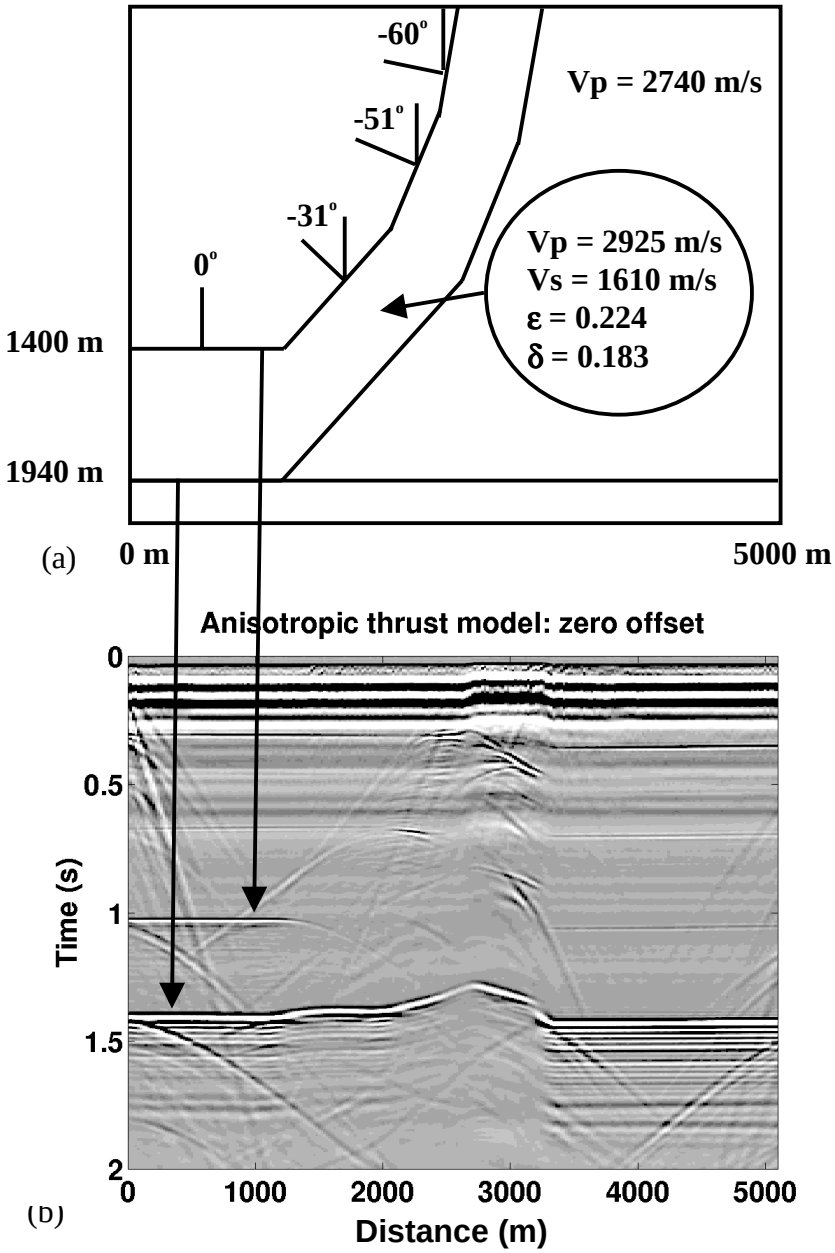

Fig. 3. Model of an anisotropic thrust sheet embedded in an isotropic background. (a) The thrust sheet is composed of 4 blocks of phenolic material (not to scale). The corresponding anisotropic parameters and axes of TI symmetry are labeled. (b) The zero-offset data. The arrows indicate the top and bottom reflections of the flat lying anisotropic block. Note the pull up of the base reflector between 1000 and 3500 m.

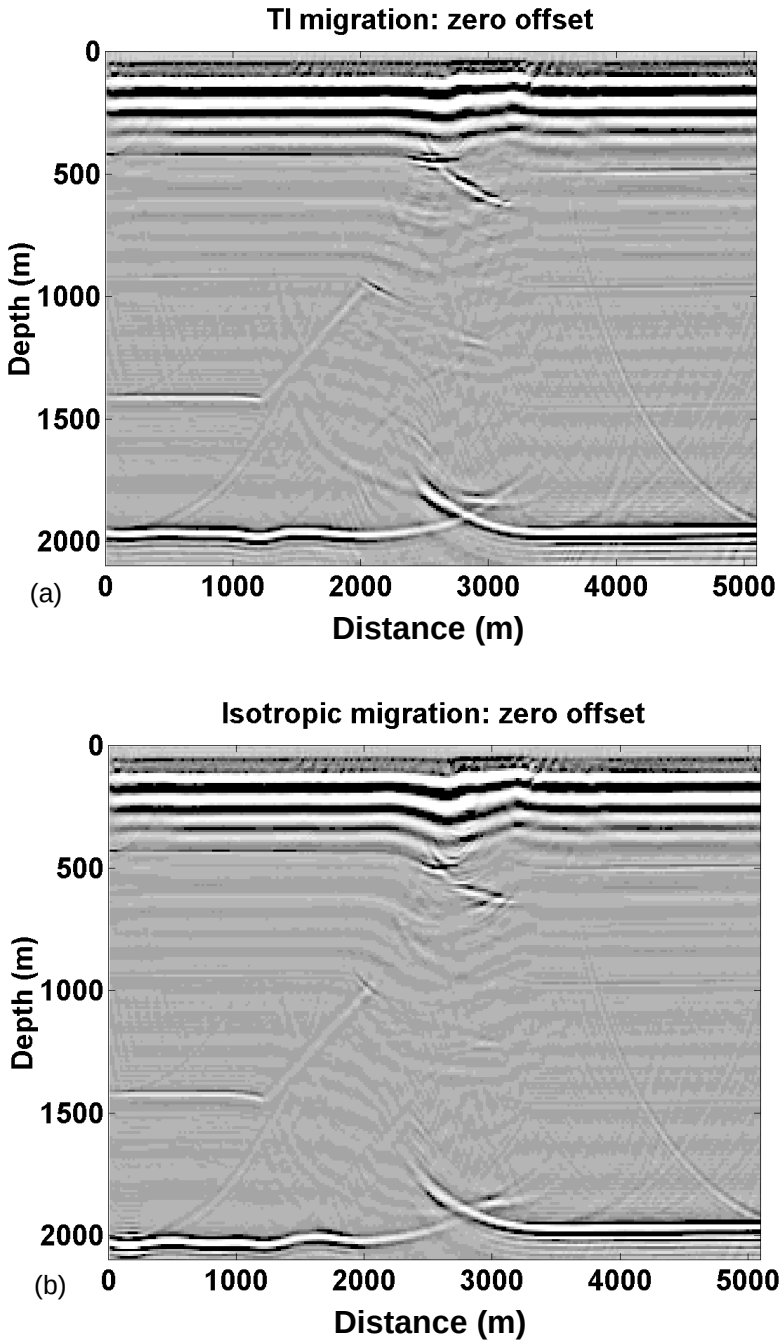

Fig. 4. Zero-offset migrations of the anisotropic thrust model (the depth scale was chosen to exaggerate differences). (a) TI migration flattens the base reflector and indicates a no data zone between 2000 and 3300 m. Isotropic incorrectly positions the base reflector (vp was chosen to be the average of the fast and slow directions = 3250 m/s). A difference in depth images (about 160 m) is apparent between base reflector under the anisotropic block and on the right.

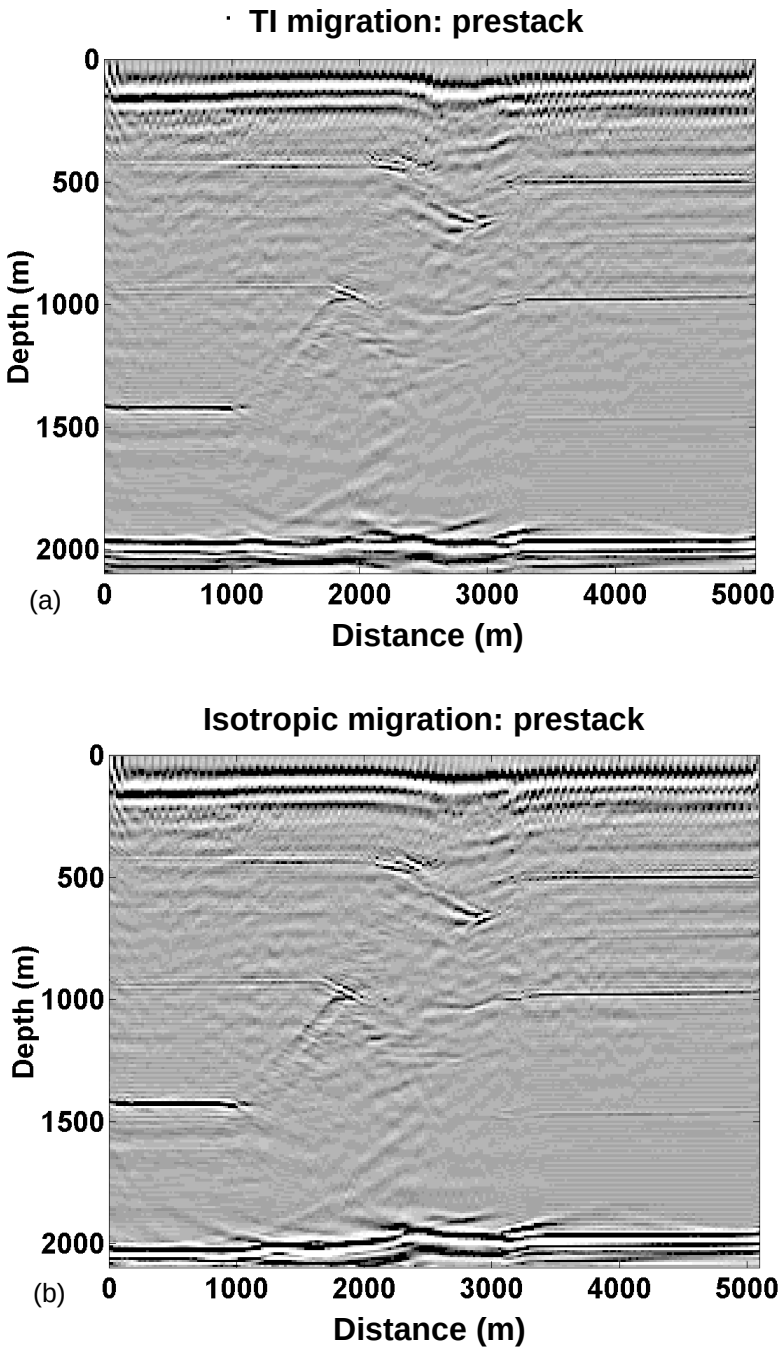

Fig. 5. Prestack migrations of the anisotropic thrust model. (a) TI migration flattens the base reflector. The scattered energy below the steepest part of the thrust sheet is due to model smoothing which was used to reduce run time. A less-smooth model would produce an even more coherent result. (b) Isotropic migration results in a stepped down image (about 160 m) of the base reflector similar to that of the zero-offset example. The base reflector beneath the steepest part of the thrust (2000 – 3000 m) is poorly imaged relative to the TI migration. The TI and isotropic migration models were equally smooth and the isotropic Vp was the average of the fast and slow directions (3250 m/s).

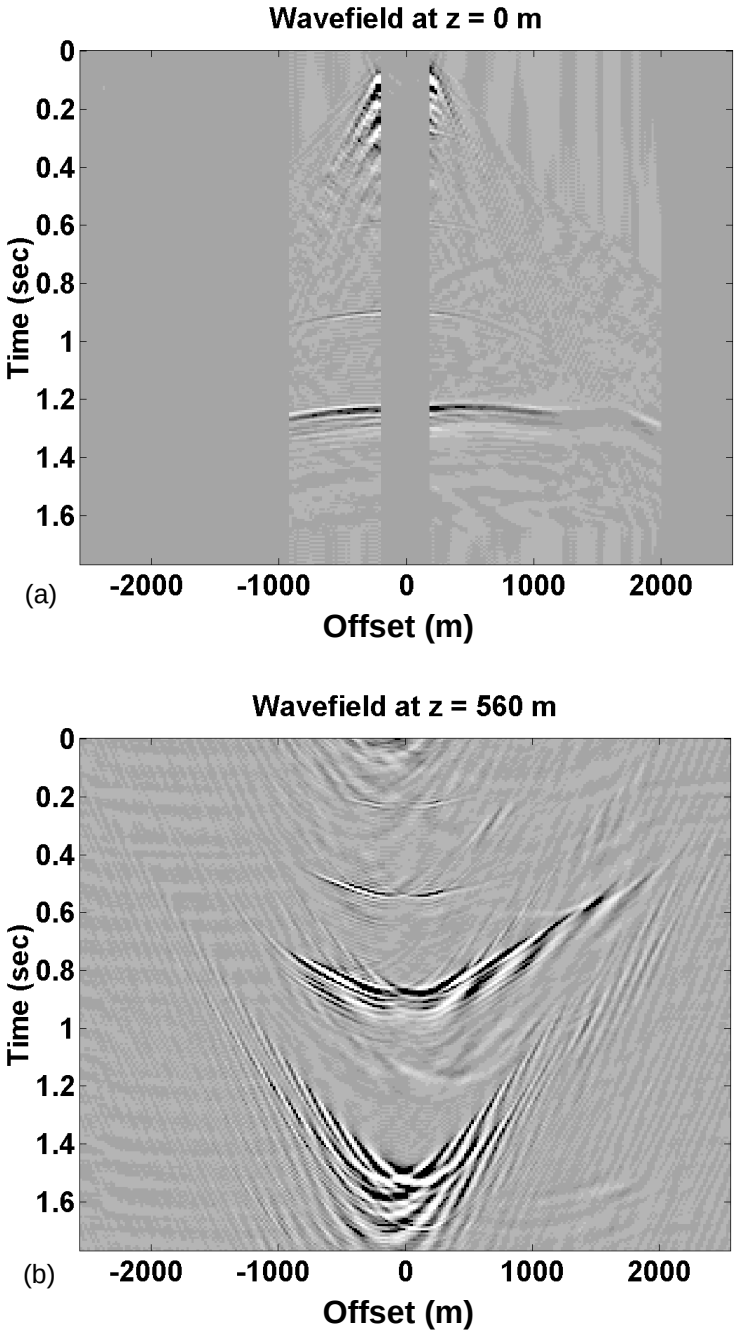

Fig. 6. Migration of a source gather. (a) A gather is input to TI source gather migration. (b) The wavefield downward continued to 560 m.

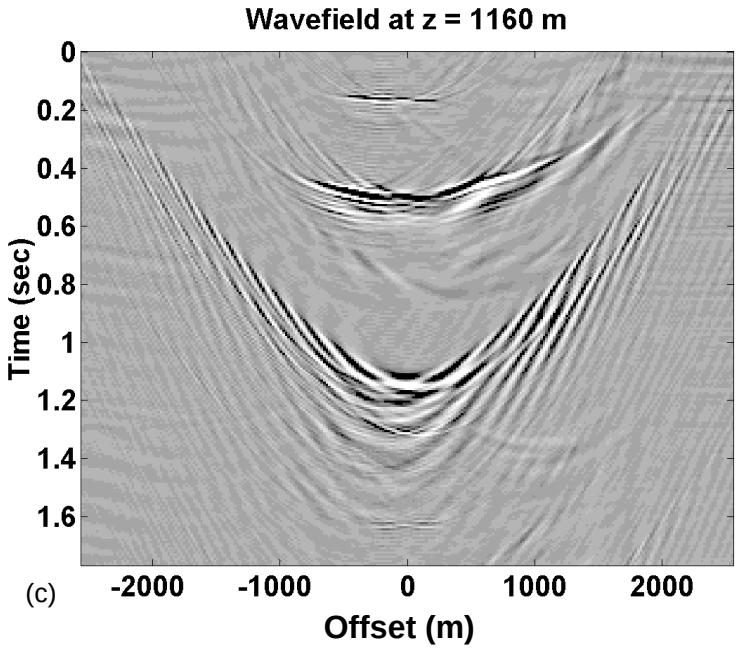

(c)

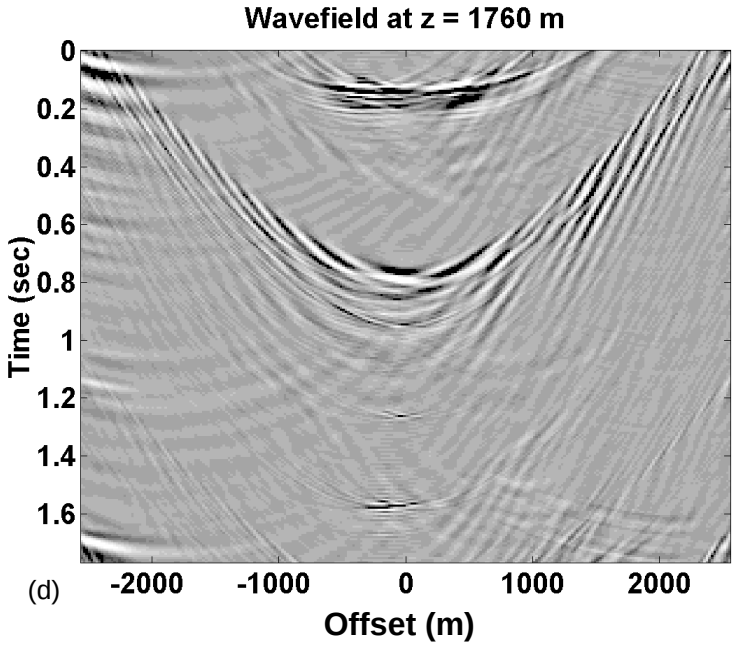

(d)

Fig. 6 cont. (c) The wavefield at 1160 m. The base reflector (t = 0.44) is continuing to focus. (d) The wavefield at 1760 m. the base reflector (t = 0.1 sec) is nearly completely focussed as it approaches t = 0 where it will be sent to output space.